Directed motion emerging from two coupled random processes: translocation of a chain through a membrane nanopore driven by binding proteins

2005 J. Phys.: Condens. Matter 17 S3945

(http://iopscience.iop.org/0953-8984/17/47/021)

INSTITUTE OF PHYSICS PUBLISHING JOURNAL OF PHYSICS: CONDENSED MATTER

J. Phys.: Condens. Matter **17** (2005) S3945–S3964 doi:10.1088/0953-8984/17/47/021

Directed motion emerging from two coupled random processes: translocation of a chain through a membrane nanopore driven by binding proteins

Tobias Ambjörnsson, Michael A Lomholt and Ralf Metzler

NORDITA—Nordic Institute for Theoretical Physics, Blegdamsvej 17, DK-2100 Copenhagen Ø, Denmark

E-mail: ambjorn@nordita.dk, mlomholt@nordita.dk and metz@nordita.dk

Received 11 July 2005
Published 4 November 2005
Online at stacks.iop.org/JPhysCM/17/S3945

Abstract

We investigate the translocation of a stiff polymer consisting of M monomers through a nanopore in a membrane, in the presence of binding particles (chaperones) that bind onto the polymer, and partially prevent backsliding of the polymer through the pore. The process is characterized by the rates: k for the polymer to make a diffusive jump through the pore, q for unbinding of a chaperone, and the rate $q\kappa$ for binding (with a binding strength κ); except for the case of no binding $\kappa = 0$ the presence of the chaperones gives rise to an effective force that drives the translocation process. In more detail, we develop a dynamical description of the process in terms of a $(2 + 1)$-variable master equation for the probability of having m monomers on the target side of the membrane with n bound chaperones at time t. Emphasis is put on the calculation of the mean first passage time τ as a function of total chain length M. The transfer coefficients in the master equation are determined through detailed balance, and depend on the relative chaperone size λ and binding strength κ, as well as the two rate constants k and q. The ratio $\gamma = q/k$ between the two rates determines, together with κ and λ, three limiting cases, for which analytic results are derived: (i) for the case of slow binding ($\gamma\kappa \to 0$), the motion is purely diffusive, and $\tau \simeq M^2$ for large M; (ii) for fast binding ($\gamma\kappa \to \infty$) but slow unbinding ($\gamma \to 0$), the motion is, for small chaperones $\lambda = 1$, ratchet-like, and $\tau \simeq M$; (iii) for the case of fast binding and unbinding dynamics ($\gamma \to \infty$ and $\gamma\kappa \to \infty$), we perform the adiabatic elimination of the fast variable n, and find that for a very long polymer $\tau \simeq M$, but with a smaller prefactor than for ratchet-like dynamics. We solve the general case numerically as a function of the dimensionless parameters λ, κ and γ, and compare to the three limiting cases.

(Some figures in this article are in colour only in the electronic version)

1. Introduction

The passage of a biopolymer (DNA, RNA, proteins) through a nanopore embedded in a membrane is one of the most crucial processes in biology, examples including the translocation of proteins through the endoplasmic reticulum, the passage of RNA through the nucleus pore membrane and the viral injection of DNA into a host, as well as DNA plasmid transport from cell to cell through cell walls [1]. Moreover, biotechnology applications of translocation processes such as rapid DNA sequencing [2, 3] and secondary structure determination of RNA [4], as well as analyte detection and nanosensing [5–7], have been discussed. Goals such as drug delivery are among the ultimate research directions connected to translocation.

Experimentally, biopolymer translocation can be probed on the single molecule level. In such experiments one commonly employs an α-haemolysin protein pore introduced into a planar lipid bilayer. But, of late, nanopores can also be created in a well defined manner by etching techniques in silicon oxide [8]. *In vitro*, translocation experiments involve either a constant driving voltage maintained during the entire measurement [3, 2]; or a high applied voltage for threading the head of the biopolymer through the pore, followed by an off-voltage and a low probe voltage [10]. Once a biopolymer enters the pore, it blocks the electrical current of ions through the pore, as monitored by patch-clamp techniques [9]. From such measurements one may directly extract, for instance, the mean translocation time τ and its dependence on applied voltage and on other physical parameters of the system. Note that cross-membrane potentials driving translocation also exist in nature [1].

Another *in vivo* mechanism is the driving by binding proteins, so-called chaperones, that appears to be particularly common for protein translocation [11–14, 17, 18], but is also implicated in the DNA transport through membranes [19, 20]. The driving of the translocation process by binding proteins constitutes a fine example of how directed motion can emerge from the coupling of two random processes. Schematically, this is illustrated in figure 1: binding proteins on the *trans* side (B) of the membrane bind non-specifically to the already translocated portion of the biopolymer. One expects three limiting dynamical regimes. (i) For slow binding (in [21] referred to as the *diffusive regime*), the relative diffusive motion of the polymer through the pore is so fast that the chaperones do not have time to bind. (ii) For fast binding but slow unbinding (the *irreversible binding regime*), the motion is ratchet-like: the chaperones bind (infinitely) fast, and while attached to the polymer they prevent backsliding through the pore, and therefore (partially) rectify the diffusive process. (iii) For the case of fast binding and unbinding dynamics (the *reversible binding regime*), one may assume that the (fast) chaperones exert an effective force originating from the chaperone chemical potential difference between the *trans* and *cis* sides [22–26]. Given the rather short biopolymer segments used in typical experimental set-ups [3] as well as short translocating biopolymers *in vivo* [1], in combination with the rather large binding interface between chaperones and driven biopolymer, non-negligible finite size effects occur, that require a modelling beyond the effective chemical potential. Such finite size effects were studied in detail in [21], finding distinct oscillations in the effective driving force. Although the different dynamical regimes above have been investigated in detail, so far no model has been able to account for all regimes and the switching in between them, as tuned by changing the physical parameters, that is possible in *in vitro* experiments. A first step towards such a unification was taken in [11] where Brownian dynamics simulation were performed, and compared to the results obtained from a $(2+1)$-variable Fokker–Planck equation.

We here extend the work in [11] and propose a $(2+1)$-variable master equation formalism for describing the full coupled dynamics of chaperone (un)binding and polymer diffusion during the translocation. In contrast to the continuum description in [11], our discrete approach

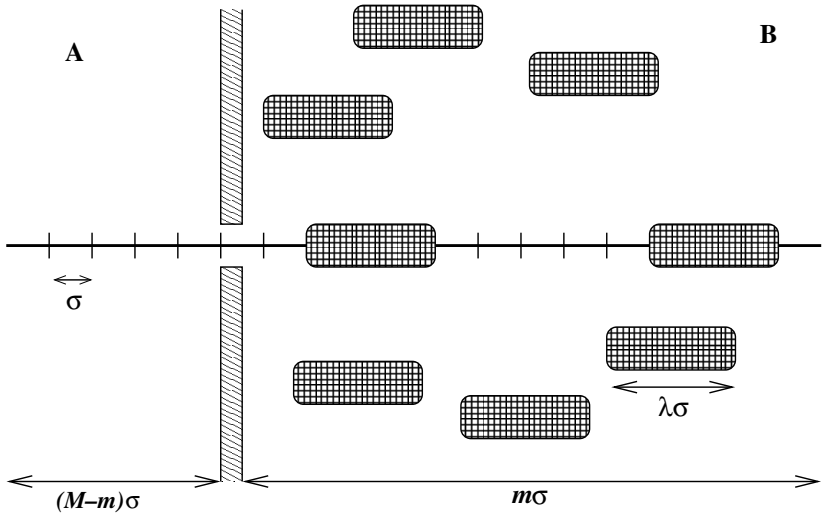

Figure 1. Schematic diagram of the translocation process: binding proteins (chaperones), of volume concentration c_0, attempt to bind to the translocating chain. Once bound, chaperones (partially) rectify the passage of the biopolymer through the nanopore. The strength of the binding between the polymer and the chaperones is characterized by the dimensionless parameter $\kappa = c_0 K^{\rm eq}$, where $K^{\rm eq}$ is the chaperone binding constant; see the text. When bound onto the polymer a single chaperone occupies a length $\lambda\sigma$, where σ is the linear monomer size (size of a base, base pair or aminoacid). The chaperones span several monomeric unit lengths, typically $\lambda \sim 10$–20. In the absence of chaperones the polymer diffuses through the pore with a diffusive rate k (the bare diffusion constant for the chain is thus $D_0 = \sigma^2 k$). The (un)binding process is characterized by an unbinding rate q for a single chaperone, leading to a competition of two random processes depending on the ratio $\gamma = q/k$.

can explicitly account for the ratchet mechanism, and include chaperones which are larger than the size of a monomer. Our approach resembles recent models developed for the coupling of the dynamics of DNA denaturation zones and selectively single-stranded DNA binding proteins [27, 28]. This general scheme allows us, as limiting cases, to consider the different regimes of fast and slow chaperone (un)binding mentioned above, including the explicit limit case of pure ratcheting. In that course, we concentrate on the effect of the chaperones, and we view the biopolymer as a stiff chain. Additional entropic effects due to the accessible degrees of freedom of the chain can be straightforwardly incorporated, as is briefly discussed. We also do not consider anomalous diffusion dynamics of very long translocating chains here [29–32]. We note that the master equation approach is a natural powerful approach to translocation dynamics (and similar random processes in systems with a discrete coordinate), as was demonstrated in [33, 34].

We finally point out three differences between our approach compared to the original Brownian ratchet ideas put forward in [14, 15].

(1) In [14, 15] the polymer motion through the pore was assumed to proceed through continuous diffusive motion until a chaperone binds; an implicit assumption in that approach is that the characteristic diffusive step length is much smaller than the size of a chaperone. In contrast, we assume that the motion proceeds through random jumps of length σ with a rate k, where σ is taken to be of the order of the length of a base, base pair or aminoacid. The two approaches are identical when all other length scales of the problem are much larger than σ; however, in our problem the size of the chaperones can be of the

order of σ, which in the general case (and in particular for the case of strong binding) alters the dynamics. The justification for our approach lies in that experimentally it is found that the mean translocation time of single-stranded DNA through an α-haemolysin pore is roughly 100 times smaller than expected including only hydrodynamic friction in the pore [23]. Also, for protein translocation the translocation times are many orders of magnitude larger than expected from simple hydrodynamic considerations [16]. These results suggest that there are strong interactions between the pore and the translocating polymer; adopting a similar explanatory description as in [23] in which the translocation process proceeds through jumps in a saw-tooth-like pore potential, our rate constant k is simply the Kramer's rate associated with a jump in this potential and σ is the distances between minima.

(2) In [14, 15] the chaperones bind independently along the polymer. Here, we include the fact that typically chaperones are larger than the size of a monomer, giving rise to a 'car parking effect' [21]—a chaperone can only bind if the space between already bound chaperones equals or is larger than the size of the chaperones; we thus extend the model in [14, 15] in order to include the fact that in general chaperones do not bind independently.

(3) We here consider arbitrary ratios of the relevant (un)binding rate and the diffusive rate k—this contrasts the results in [14, 15] where only the cases of Brownian ratchet motion and fast (un)binding dynamics were considered.

We will point out similarities and differences between our approach and that in [14, 15] as they arise throughout the text.

2. Master equation for chaperone-driven translocation

Let us consider the general translocation dynamics for a chain of length $M\sigma$, where σ is the typical linear monomer (base, base-pair, aminoacid) size. The coordinates we choose for the description of the chaperone-driven biopolymer passage are the number m of monomers of the chain on the *trans* side B (the number of monomers on the *cis* side A is then $M - m$) and the number n of bound chaperones, see figure 1. The size of the binding interface of a chaperone bound to the biopolymer is $\lambda\sigma$. No chaperones are assumed to be present on side A. Due to inherent thermal fluctuations the variables m and n are stochastic variables and the aim is to understand the temporal behaviour of these variables; below we use a master equation formulation for the associated probability distribution. This description rests on the assumption that all other variables in the system are fast in comparison to the rate of change of the coordinates m and n. From the solution of this master equation any experimental observable can be calculated. Here, the main quantity of interest is the mean first passage time $\tau(M)$ as a function of the chain length M and chaperone size λ, as well as of two dimensionless parameters introduced in section 4: the binding strength κ and the ratio γ between the rate k associated with making a diffusive step and the rate q for chaperone unbinding. In our description, the size of the pore and the number of monomers present in the pore at a given time enters only through the effective rate k (see [35, 23, 33, 34, 36] for more detailed investigations of the effects of finite-sized pores).

Denote by $P(m, n, t|m', n')$ the conditional probability density of finding m monomers of the chain on side B (the already translocated distance in units of monomers) with n bound chaperones at time t, provided that at the initial time the system was in a state with $m = m'$ and $n = n'$. With the short-hand notation $P(m, n, t) = P(m, n, t|m', n')$, the time evolution of $P(m, n, t)$ is governed by the $(2 + 1)$-variable master equation [37]

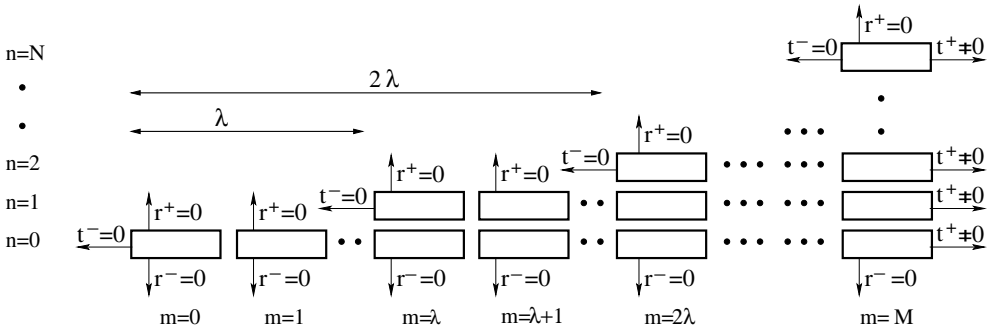

Figure 2. Configuration lattice spanned by translocation coordinate m and number n of bound chaperones, with allowed configuration states of the system (□). Each time m reaches a multiple of λ, an additional chaperone can bind. The scheme also indicates forbidden jumps.

$$\begin{aligned}\frac{\partial P(m,n,t)}{\partial t} &= \mathsf{t}^{+}(m-1,n)P(m-1,n,t)+\mathsf{t}^{-}(m+1,n,t)P(m+1,n,t)\\ &\quad-\left[\mathsf{t}^{+}(m,n)+\mathsf{t}^{-}(m,n)\right]P(m,n,t)\\ &\quad+\mathsf{r}^{+}(m,n-1)P(m,n-1)+\mathsf{r}^{-}(m,n+1)P(m,n+1,t)\\ &\quad-\left[\mathsf{r}^{+}(m,n)+\mathsf{r}^{-}(m,n)\right]P(m,n,t).\end{aligned} \tag{1}$$

The transfer coefficients $\mathsf{t}^{\pm}$ represent the rates for a change in the translocation coordinate m and the coefficients $\mathsf{r}^{\pm}$ specify the (un)binding of chaperones, i.e., a change in n; both transfer coefficients are explicitly defined in section 4.[1] Equation (1) is subject to the general initial condition $P(m,n,t=0|m',n')=\delta_{m,m'}\delta_{n,n'}$, where δ_{z_1,z_2} denotes the Kronecker delta. Here, we assume that $m'=0$ and $n'=0$:

$$P(m,n,0)=\delta_{m,0}\delta_{n,0}, \tag{2}$$

i.e., that initially the chain is fully on side A, with its head just in the pore (and therefore has no bound chaperones), corresponding to the typical situation *in vitro* and *in vivo*.

We now consider the boundary conditions that must be imposed on the transfer coefficients. Once the chain has arrived completely on side B, i.e., $m=M$, we assume that it cannot find its way back into the pore. We impose, that is, the absorbing boundary condition[2]

$$\mathsf{t}^{-}(M+1,n)=0. \tag{3}$$

For the absorbing condition (3) imposed here, the Mth transfer coefficient $\mathsf{t}^{+}(M,n)$ in general is finite, giving rise to jumps out from the configuration lattice (see figure 2), such that in this case $\sum_{m,n}P(m,n,t)$ decreases with time, and therefore $P(m,n,t)$ is an improper probability distribution. At $m=0$, we impose the reflecting boundary condition

$$\mathsf{t}^{-}(0,0)=0. \tag{4}$$

[1] For equation (1) to be completely specified we need to describe the transfer coefficients just outside the configuration lattice (illustrated in figure 2) as well:

$$\mathsf{t}^{-}(m=M+1,n)=\mathsf{t}^{+}(m=j\lambda-1,n=n^{\max}(m+1))=0$$

for integer j, and

$$\mathsf{r}^{+}(m,n=-1)=\mathsf{r}^{-}(m,n=n^{\max}(m)+1)=0.$$

[2] We note that a reflecting boundary condition at $m=M$, as occurring for instance in the description of DNA-breathing dynamics [27, 28], would have the structure $\mathsf{t}^{+}(M,n)=0$.

This condition guarantees that the chain does not retract from the pore to side A. Additionally, we require that the chain cannot move towards side A, when it is fully occupied with chaperones:

$$\mathsf{t}^{-}\left(m = n^{\max}(m)\lambda, n^{\max}(m)\right) = 0, \tag{5}$$

where

$$n^{\max}(m) = [m/\lambda] \tag{6}$$

is the maximum number of bound chaperones for a given m (and $[\cdot]$ is the Landau bracket returning the integer value of the argument). The boundary condition (5) is crucial for the emergence of ratchet motion as discussed in section 5.2. For the (un)binding rates, we have the natural condition

$$\mathsf{r}^{-}(m, 0) = 0, \tag{7}$$

stating that no further unbinding can occur once the chain is empty of chaperones. Similarly, chaperones cannot bind to a fully occupied chain:

$$\mathsf{r}^{+}\left(m, n^{\max}(m)\right) = 0. \tag{8}$$

The configuration lattice on which the jump dynamics, as defined by equation (1) and the transfer coefficients $\mathsf{t}^{\pm}$ and $\mathsf{r}^{\pm}$, is schematically shown in figure 2, together with the boundary conditions above.

For internal points on the lattice in figure 2 the transfer coefficients are constrained (but not fully determined) by the detailed balance condition [37]. For our specific system, the detailed balance condition takes on the structure (compare to [27, 28])

$$\mathsf{t}^{+}(m-1, n)\mathscr{Z}(m-1, n) = \mathsf{t}^{-}(m, n)\mathscr{Z}(m, n) \tag{9}$$

and

$$\mathsf{r}^{+}(m, n-1)\mathscr{Z}(m, n-1) = \mathsf{r}^{-}(m, n)\mathscr{Z}(m, n) \tag{10}$$

where $\mathscr{Z}(m, n)$ is the partition coefficient for a given m and n. Whereas equation (10) holds for all n, equation (9) only holds for $0 \leqslant m \leqslant M$, and not for $m = M + 1$. This is due to the fact that $\mathsf{t}^{+}(M, n) \neq 0$, corresponding to our absorbing boundary condition; in the case of a reflecting boundary condition, $\mathsf{t}^{+}(M, n) = 0$, detailed balance would be fulfilled for all m, and for long times $P(m, n, t)$ would reach the stationary density:

$$P^{\mathrm{st}}(m, n) = \mathscr{Z}(m, n)/\mathscr{Z} \tag{11}$$

where $\mathscr{Z} = \sum_{m,n}\mathscr{Z}(m, n)$. Here, in contrast, our absorbing condition provides that $P(m, n, t \to \infty) = 0$, and $P(m, n, t)$ is in fact an improper probability distribution. An explicit expression for $\mathscr{Z}(m, n)$ and for physically realistic transfer coefficients, satisfying the detailed balance conditions above, is given in section 4.

The general solution to the master equation (1) can be decomposed into the eigenmodes according to

$$P(m, n, t) = P(m, n, t|m', n') = \sum_{p} c_p(m', n')Q_p(m, n)\mathrm{e}^{-\eta_p t}, \tag{12}$$

where the expansion coefficients $c_p(m', n')$ are determined by the initial condition. Inserting the above expansion into equation (1) produces the eigenvalue equation

$$\begin{aligned}
&\mathsf{t}^{+}(m-1, n)Q_p(m-1, n) + \mathsf{t}^{-}(m+1, n)Q_p(m+1, n)\\
&\quad - \left[\mathsf{t}^{+}(m, n) + \mathsf{t}^{-}(m, n)\right]Q_p(m, n)\\
&\quad + \mathsf{r}^{+}(m, n-1)Q_p(m, n-1) + \mathsf{r}^{-}(m, n+1)Q_p(m, n+1)\\
&\quad - \left[\mathsf{r}^{+}(m, n) + \mathsf{r}^{-}(m, n)\right]Q_p(m, n) = -\eta_p Q_p(m, n)
\end{aligned} \tag{13}$$

for the pth eigenmode, with eigenvalues η_p and eigenfunctions $Q_p(m,n)$. We label the eigenvalues such that $0 < \eta_0 < \eta_1 < \eta_2 \cdots < \eta_M$. We note that all η_p are real and positive (see appendix A and [38, 39]), which guarantees that $P(m,n,t \to \infty) = 0$, as it should for an ergodic system with a sink (see equation (3)). The eigenvectors $Q_p(m,n)$ satisfy the orthonormality relation given in equation (A.4). We prefer using an eigenvalue approach (spectral representation) to the present problem rather than solving the master equation in real time, since the eigenvalue approach avoids time discretization problems.

3. Mean first passage time of translocation

We here derive an expression for the mean first passage time of translocation, i.e., the mean time it takes the biopolymer, while being driven by chaperone (un)binding, to fully cross the membrane pore. We will determine the mean first passage time as a function of the eigenvalues η_p and the eigenfunctions $Q_p(m,n)$ defined through equation (13).

As before, denote by $P(m,n,t|m',n')$ the conditional probability to find the system in state (m,n) at time t, given the initial condition (m',n') at time $t = 0$. Then the (survival) probability that the absorbing boundary at $m = M+1$ has not yet been reached up to time t is

$$\mathscr{S}(m',n',t) = \sum_{m=0}^{M} \sum_{n=0}^{n^{\max}(m)} P(m,n,t|m',n'). \tag{14}$$

The probability that the absorbing boundary is reached within the time interval $[t, t+\mathrm{d}t]$ is

$$\begin{aligned} f(m',n',t)\,\mathrm{d}t &= \mathscr{S}(m',n',t) - \mathscr{S}(m',n',t+\mathrm{d}t) \\ &= -\left(\frac{\partial}{\partial t}\mathscr{S}(m',n',t)\right)\mathrm{d}t. \end{aligned} \tag{15}$$

This expression is positive, as $\mathscr{S}$ is decreasing with time. From the first passage time density $f(m',n',t)$, the mean first passage time thus follows by integration:

$$\mathsf{T}(m',n') = \int_0^\infty t f(m',n',t)\,\mathrm{d}t = \int_0^\infty \mathscr{S}(m',n',t)\,\mathrm{d}t. \tag{16}$$

To express the mean first passage time T in terms of the eigenvalues and eigenfunctions, we introduce the eigenmode expansion (12) into equation (16), yielding

$$\begin{aligned} \mathsf{T}(m',n') &= \sum_{m,n} \int_0^\infty \sum_p c_p(m',n') Q_p(m,n) \mathrm{e}^{-\eta_p t}\,\mathrm{d}t \\ &= \sum_p \eta_p^{-1} \frac{Q_p(m',n')}{P^{\mathrm{st}}(m',n')} \sum_{m,n} Q_p(m,n) \end{aligned} \tag{17}$$

where $P^{\mathrm{st}}(m,n)$ is given in equation (11). We have above made use of the orthonormality relation (A.4) in order to express $c_p(m',n')$ in terms of the initial probability density $P(m,n,0|m',n')$, and used the fact that this general initial condition takes the explicit form $P(m,n,0|m',n') = \delta_{m,m'}\delta_{n,n'}$. Equation (17) is the discrete counterpart of the continuous result derived in [38], and expresses the mean first passage time (for any given initial condition, specified by m' and n') in terms of the eigenvalues and eigenvectors of equation (13).

Using the general result (17) together with the special initial condition (2) considered here, we see that the mean translocation time for a polymer starting with its head in the pore becomes

$$\mathsf{T} = \mathsf{T}(0,0) = \sum_p \mathsf{T}_p \eta_p^{-1}, \tag{18}$$

with

$$\tau_p = \frac{Q_p(0,0)}{P^{\rm st}(0,0)} \sum_{m,n} Q_p(m,n). \tag{19}$$

The mean translocation time is thus obtained by summing up the relaxation times η_p^{-1} with weight factors τ_p, in turn being determined by the eigenfunctions $Q_p(m,n)$.

4. Partition function and transfer rates

The partition coefficient $\mathscr{Z}(m,n)$ appearing in the detailed balance conditions (9) and (10) constrain, but do not fully specify, the transfer coefficients $\mathsf{t}^{\pm}(m,n)$ and $\mathsf{r}^{\pm}(m,n)$. In this section we give explicit expressions for both the partition coefficient as well for the transfer coefficients.

For a given value of translocation coordinate m and a given number of bound chaperones n the partition coefficient is

$$\mathscr{Z}(m,n) = \mathscr{Z}^{\rm poly}(m)\,\mathscr{Z}^{\rm chap}(m,n), \tag{20}$$

corresponding to the product of the partition coefficients $\mathscr{Z}^{\rm poly}(m)$ of the undressed biopolymer and $\mathscr{Z}^{\rm chap}(m,n)$ of the chaperone (un)binding, which in turn depends on the translocation coordinate m defining the number of accessible binding sites; see figure 1. The polymeric factor $\mathscr{Z}^{\rm poly}(m)$ measures the accessible degrees of freedom (or better, their confinement) of the biopolymer chain threading through the pore. For a flexible chain, this would invoke the critical exponent for a polymer grafted to a surface [24]. Single-stranded DNA or RNA would qualify for such a description. Double-stranded DNA and proteins are more of a semiflexible nature, and corrections to the scaling behaviour would ensue. Moreover, the interactions between chain and pore are not fully known; compare the discussions in [10, 34]. For simplicity, and to solely concentrate on the chaperone effects, we assume our chain to be completely stiff, so that

$$\mathscr{Z}^{\rm poly}(m) = 1. \tag{21}$$

Note, however, that any expression for $\mathscr{Z}^{\rm poly}(m)$ can easily be implemented through the numerical formalism discussed below, provided that the chaperone binding does not depend on the curvature of the polymer.

The second factor in the partition function $\mathscr{Z}(m,n)$, the contribution $\mathscr{Z}^{\rm chap}(m,n)$ from chaperone (un)binding,

$$\mathscr{Z}^{\rm chap}(m,n) = \kappa^n \Omega^{\rm chap}(m,n) \tag{22}$$

combines the n-fold gain of the binding energy, entering through the factor κ^n, with the number of possible ways of arranging n proteins along m biopolymer monomers,

$$\Omega^{\rm chap}(m,n) = \binom{m-(\lambda-1)n}{n} = \frac{(m-[\lambda-1]n)!}{n!(m-\lambda n)!}, \tag{23}$$

compare [41, 42, 28, 21]. Here, we also introduced the binding strength

$$\kappa = c_0 K^{\rm eq}, \tag{24}$$

that, in turn, depends on the chaperone concentration c_0 in the surrounding solution and the equilibrium binding constant $K^{\rm eq} = v_0 \exp(|E_{\rm bind}|/k_{\rm B}T)$ with the typical volume v_0 of the chaperones; $E_{\rm bind}$ is the chaperone binding energy; $\beta = 1/k_{\rm B}T$ with $k_{\rm B}$ being the Boltzmann constant and T the temperature.

The transfer rates $\mathsf{t}^{\pm}(m,n)$ and $\mathsf{r}^{\pm}(m,n)$ governing the transitions $m \to m \pm 1$ and $n \to n \pm 1$ in the master equation (1) are subject to the detailed balance conditions (9) and (10). Here, we seek concrete expressions for the rates. For the forward translocation rate $\mathsf{t}^{\pm}$, we solely observe the influence of the polymeric degrees of freedom. We assume that the rate limiting step for the polymer motion originates from interactions in the pore [23] and choose the form

$$\mathsf{t}^{+}(m,n) = k\frac{\mathscr{Z}^{\mathrm{poly}}(m+1)}{\mathscr{Z}^{\mathrm{poly}}(m)} = k = \mathsf{t}^{+}(m). \tag{25}$$

It simplifies to the constant rate k due to the assumption of a stiff chain, $\mathscr{Z}^{\mathrm{poly}}(m) = 1$, where k is the rate for making a diffusive jump of length σ; see the introduction and figure 1. Conversely, for the backward rate, we specify

$$\mathsf{t}^{-}(m,n) = k\frac{\mathscr{Z}(m-1,n)}{\mathscr{Z}(m,n)} = k\frac{\mathscr{Z}^{\mathrm{chap}}(m-1,n)}{\mathscr{Z}^{\mathrm{chap}}(m,n)} = k\frac{\Omega^{\mathrm{chap}}(m-1,n)}{\Omega^{\mathrm{chap}}(m,n)}. \tag{26}$$

In the case of the $\mathsf{t}^{\pm}$, we thus choose that while the forward rate is independent of the number of bound chaperones and their configurations, the sliding of the chain toward the *cis* side A of the membrane will, in general, be opposed by bound proteins, $\mathsf{t}^{-}(m,n) \leqslant k$. We have chosen t^{-} such that it is proportional to the probability $\Omega^{\mathrm{chap}}(m-1,n)/\Omega^{\mathrm{chap}}(m,n)$ that the binding site closest to the pore on side B is vacant. In the limit $n = 0$, both forward and backward rates are identical: $\mathsf{t}^{+}(m,n=0) = \mathsf{t}^{-}(m,n=0) = k$, and we have pure, unbiased diffusion with a bare diffusion constant $D_0 = \sigma^2 k$,[3] as it should be. We point out that whenever the polymer is not fully occupied, the binding proteins may, in general, slide along the DNA [43], thereby possibly exploring the different bound chaperone configurations on a faster timescale. Such sliding motion was present in the Brownian simulations in [11].

For the transfer coefficients associated with chaperone (un)binding we specify

$$\begin{aligned}\mathsf{r}^{+}(m,n) &= (n+1)q\frac{\mathscr{Z}^{\mathrm{chap}}(m,n+1)}{\mathscr{Z}^{\mathrm{chap}}(m,n)} \\ &= k\gamma\kappa\frac{(n+1)\Omega^{\mathrm{chap}}(m,n+1)}{\Omega^{\mathrm{chap}}(m,n)};\end{aligned} \tag{27}$$

$$\mathsf{r}^{-}(m,n) = nq = k\gamma n. \tag{28}$$

To make comparison with the chaperone unbinding rate q easier, we introduced here the dimensionless ratio

$$\gamma = \frac{q}{k} \tag{29}$$

between the unbinding rate q of a single chaperone (for $n = 1$ we have $\mathsf{r}^{-} = q$) and the diffusive rate k. We have chosen r^{+} to be proportional to the number of ways $\mathscr{N} = (n+1)\Omega^{\mathrm{chap}}(m,n+1)/\Omega^{\mathrm{chap}}(m,n)$ of adding one additional chaperone if there are already n bound. In the general case $\mathscr{N}$ includes a 'car parking effect' [41, 21], i.e., the fact that a chaperone can only bind in between two chaperones which are separated by a distance equal to or larger than the chaperone size. In the limit $\lambda = 1$ we have independent binding and the resulting expression becomes $\mathscr{N} = m - n$ as it should, and r^{+} is thus proportional to the number of free binding sites; compare the discussion in [28, 37]. We note that r^{+} depends linearly on the volume concentration c_0 of chaperones (compare [11]) through the parameter $\kappa = c_0 K^{\mathrm{eq}}$, where K^{eq} is the binding constant as before. Conversely, the unbinding rate is simply proportional to the number of chaperones bound to the biopolymer (as it should

[3] The bare diffusion constant D_0 should not be confused with the effective diffusion constant relevant for general driven motion over distances much larger than σ, see [23].

be [37]) and independent of the concentration of chaperones. A word on the choice of this asymmetric form is in order. To put the full effect of chaperone concentration and binding energy contained in $\mathscr{L}^{\rm chap}$ into the binding rate r^+, and therefore leave the unbinding rate r^- unaffected corresponds to the physical picture that the unbinding process should solely depend on the dissociation of local bonds. It should also be noted that cooperative binding of chaperones can in principle be included in our formalism [21].

The explicit expressions (25)–(28) for the transfer coefficients, together with the boundary conditions in equations (4), (5), (7) and (8), completely determine the translocation/chaperone (un)binding dynamics through the master equation (1) or the associated eigenvalue equation (13). In the next section we solve these equations in order to obtain the mean translocation time, using expression (18) derived in the previous section.

5. General and limiting results

In this section we obtain results for the mean translocation time for different physical parameters. In particular three cases can be distinguished: (i) slow chaperone binding, leading to unbiased pure diffusion for a finite translocating chain; (ii) fast chaperone binding but slow unbinding, leading to a pure chaperone-mediated ratchet motion; and (iii) fast chaperone (un)binding dynamics, tractable via adiabatic elimination, leading to a one-variable effective force; compare figure 3. This analytical treatment is complemented with (iv) numerical analysis. We stop to note that the emergence of the three limiting cases from a general scheme is the major advantage of the approach pursued herein in comparison to the one-dimensional treatment in [21], which explicitly accounts for case (iii) above only.

5.1. Slow binding dynamics, $\gamma\kappa \to 0$

Slow chaperone binding is prevalent when the dimensionless ratio $\gamma\kappa \to 0$, as in this limit we have that $\mathsf{r}^+(m,n) \to 0$ (see equation (27)). Experimentally one can reach small values of κ and hence the slow binding regime, by sufficiently low chaperone concentration c_0 or for small binding energy $E_{\rm bind}$, see equation (24). As initially $n = 0$ (see equation (2)), the dynamics is fully described by the transfer coefficients

$$\mathsf{t}^+(m,0) = \mathsf{t}^-(m,0) = k, \tag{30}$$

together with the reflecting boundary (compare equation (4))

$$\mathsf{t}^-(0,0) = 0 \tag{31}$$

and the absorbing boundary condition (see equation (3))

$$\mathsf{t}^-(M+1,0) = 0. \tag{32}$$

We see from equation (30) that in the slow binding limit the rate for a forward step equals the backward rate and therefore the motion is purely diffusive for a finite chain. Making use of the general expression for the mean first passage time for one-dimensional motion contained in equation (B.1) we arrive at

$$\mathsf{T} = \mathsf{T}_{\rm diff} = \sum_{m=0}^{M}\sum_{m'=0}^{m} k^{-1} = k^{-1}\left[(M+1)\left(1+\frac{M}{2}\right)\right]. \tag{33}$$

For large M, the mean first passage time thus scales like $\mathsf{T} \simeq M^2/2k$, as it should for a purely diffusive first passage process. In terms of the bare diffusion constant $D_0 = \sigma^2 k$ and the chain length $L = M\sigma$ we have $\mathsf{T} \simeq L^2/2D_0$ in agreement with [14, 15, 11]. The diffusive motion

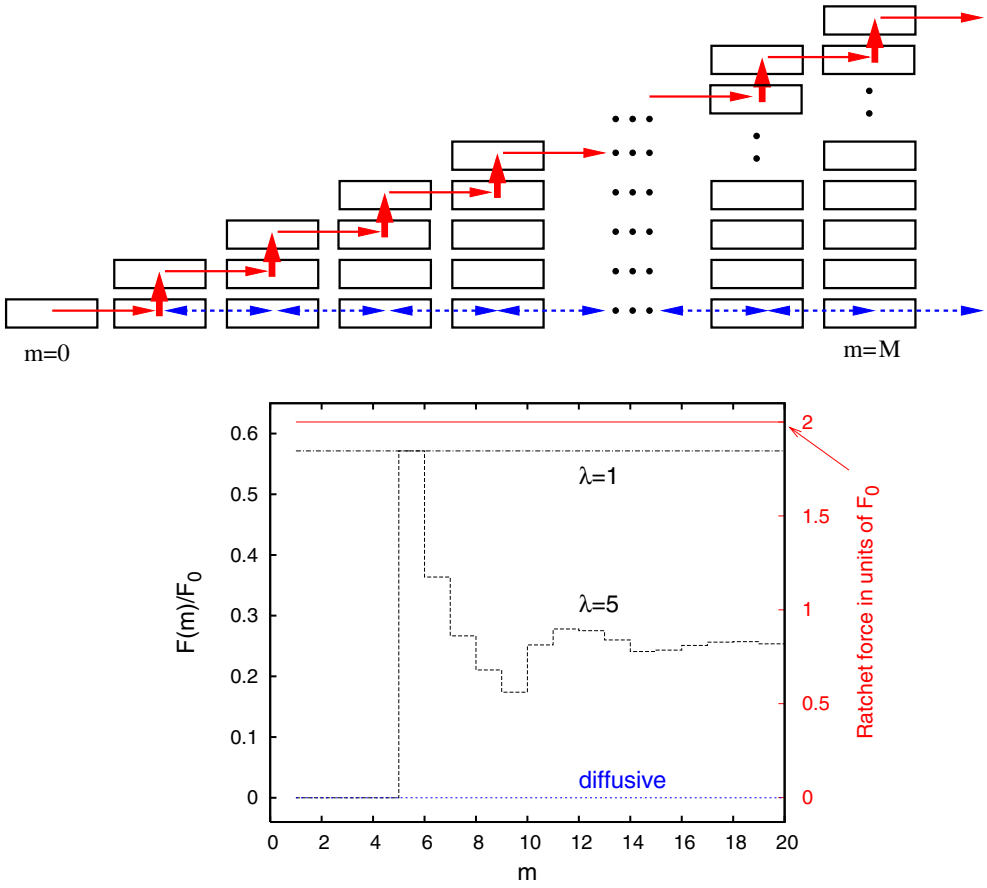

Figure 3. Top: schematic diagram of the analytically tractable limiting cases of the coupled translocation–chaperone (un)binding dynamics. (i) The dashed (blue) arrows indicate the purely, unbiased, diffusive motion for slow binding. (ii) The solid (red) arrows indicate the translocation dynamics for ratchet motion in the case of fast chaperone binding. Notice that for these two cases only a small part of the phase space is explored before the polymer is absorbed at $m = M + 1$. In contrast, for (iii) the fast (un)binding case, the entire phase space is explored before absorption. Bottom: effective force $F(m)$ for the three limiting regimes above. For (i) diffusive motion we have $F(m) \equiv 0$ ((blue) dashed line); for (ii) ratchet motion we effectively have $F(m) = 2F_0$ ((red) solid line referring to the right ordinate), with a characteristic force $F_0 = k_B T/\sigma$; for (iii) fast (un)binding we have $F(m) = 2F_0(\tilde{t}^+(m) - \tilde{t}^-(m))/(\tilde{t}^+(m) + \tilde{t}^-(m))$ where $\tilde{t}^{\pm}(m)$ are defined in section 5.3. We here use a binding strength $\kappa = 0.8$, and two different chaperone sizes $\lambda = 1$ (the upper dash–dotted line) and $\lambda = 5$ (the lower dashed curve). Note that the onset of a non-zero force is at $m = \lambda$, i.e. the force is zero unless there are sufficiently many monomers to accommodate at least one chaperone. Also notice the oscillations in the force for the case $\lambda = 5$. We point out that the forces above are not explicitly used in the dynamical scheme, but are convenient for illustrative purposes.

on the general configuration lattice is schematically illustrated by the blue dashed arrows in figure 3 (top). Notice that due to the slow binding only a small part of the phase space is explored before the polymer is absorbed. It is sometimes useful to picture the dynamics as jump motion in a force field; for purely diffusive motion we have a force $F(m) \equiv 0$, i.e. the force is zero, as schematically illustrated in figure 3 (bottom). In figure 5 the mean translocation time (33) is shown and compared to the different cases discussed in the remaining part of this section.

5.2. *Fast binding but slow unbinding, $\gamma \to 0$, $\gamma\kappa \to \infty$ and $\lambda = 1$: ratchet motion*

As the effective rate γ and the binding strength can be chosen independently, we can specify them such that we encounter slow unbinding designated by $\gamma \to 0$ but fast binding, $\gamma\kappa \to \infty$. For small chaperones, $\lambda = 1$ (univalent binding), this corresponds to the stepwise transitions marked by the solid (red) arrows in figure 3. Each time a monomer of the biopolymer exits from the membrane pore towards the *trans* side, it is immediately occupied by a chaperone. The irreversibly bound chaperones do not unbind and prevent backwards motion (see equation (5)) so that the motion becomes unidirectional with effective rates $\bar{\mathsf{t}}^{+}(m) = k$ and $\bar{\mathsf{t}}^{-}(m) = 0$. The general master equation (1) then reduces to the effective $(1+1)$-variable equation

$$\frac{\partial \overline{P}(m)}{\partial t} = k\left[\overline{P}(m-1,t) - \overline{P}(m,t)\right], \tag{34}$$

where we introduced the short-hand notation $\overline{P}(m,t) = P(m, n^{\max}(m), t)$. The process is that of taking $M+1$ forward steps with a rate per step k, and the mean first passage time therefore becomes

$$\tau = \tau_{\text{ratchet}} = k^{-1}(M+1). \tag{35}$$

Thus, τ scales linearly with M for large M in this ratchet limit. The mean translocation time (35) is shown in figure 5. Equations of the same form as (34) also occur in the theoretical description of shot noise, and correspond to the forward mode of the wave equation. For ratchet motion we define an effective force $F(m) = 2F_0(\bar{\mathsf{t}}^{+}(m) - \bar{\mathsf{t}}^{-}(m))/(\bar{\mathsf{t}}^{+}(m) + \bar{\mathsf{t}}^{-}(m)) = 2F_0$, where $F_0 = k_{\mathrm{B}}T/\sigma$; the effective force associated with ratchet motion is thus constant, as schematically shown in figure 3 (bottom).

Comparing equations (33) and (35) we see that $\tau_{\text{ratchet}}/\tau_{\text{diff}} = 2/M$ for large M. This result contrasts with the results of a Brownian ratchet [14, 15] for which the same quantity equals $1/M$. This difference originates from the fact that here the size of a chaperone equals the diffusive step length σ, whereas in the Brownian ratchet $\sigma \to 0$ (continuous diffusion versus our stepwise diffusion), but with a finite chaperone size[4].

5.3. *Fast (un)binding dynamics, $\gamma \to \infty$ and $\gamma\kappa \to \infty$*

Finally, we address the case of fast binding, $\gamma\kappa \to \infty$, and fast unbinding, $\gamma \to \infty$. Under these conditions, it is possible to adiabatically eliminate the fast variable n [28, 39], resulting in the effective forward and backward rates

$$\bar{\mathsf{t}}^{\pm}(m) = \sum_{n=0}^{n^{\max}(m)} \mathsf{t}^{\pm}(m,n)\frac{\mathscr{Z}(m,n)}{\mathscr{Z}(m)}. \tag{36}$$

For a stiff polymer, implying $\mathsf{t}^{+}(m,n) = k$ (see equation (25)), we obtain the following simple expression for the forward rate: $\bar{\mathsf{t}}^{+}(m) = k$. When calculating the backward rate $\bar{\mathsf{t}}^{-}(m)$ one should remember to incorporate the boundary rates as given in equation (5). Here, in general, $\mathscr{Z}(m) = \mathscr{Z}^{\text{poly}}(m)\mathscr{Z}^{\text{chap}}(m)$, and

$$\mathscr{Z}^{\text{chap}}(m) = \sum_{n=0}^{n^{\max}(m)} \mathscr{Z}^{\text{chap}}(m,n). \tag{37}$$

[4] The results from [14, 15] can be recovered if we imagine the chaperones in the ratchet case to be fast binding but immobile after binding. We would then expect the mean first passage time for $M \gg \lambda \gg 1$ to be the sum of M/λ diffusive mean first passage times $k^{-1}\lambda^2/2$. Thus the ratio with the purely diffusive mean first passage time in equation (33) would become $\tau_{\text{ratchet}}/\tau_{\text{diff}} = \lambda/M$ in agreement with [14, 15].

Making use of the fact that the transfer coefficients satisfy the detailed balance condition, $\bar{t}^+(m-1)\mathscr{Z}(m-1) = \bar{t}^-(m)\mathscr{Z}(m)$ (see [28]) so that we can use equation (B.3), we obtain the mean first passage time

$$\tau = \sum_{m=0}^{M} \frac{1}{\bar{t}^+(m)\mathscr{Z}(m)} \sum_{m'=0}^{m} \mathscr{Z}(m') = k^{-1} \sum_{m=0}^{M} \frac{1}{\mathscr{Z}(m)} \sum_{m'=0}^{m} \mathscr{Z}(m'), \tag{38}$$

where we have used that here $\bar{t}^+(m) = k$. The sum in (38) can straightforwardly be numerically evaluated and the resulting mean translocation time is shown in figure 5.

In order to simplify the mean translocation time (38) further for large chain lengths M, a knowledge of the partition function $\mathscr{Z}(m)$ for large m suffices. Instead of the combinatorial approach given in the previous subsections, the partition function for large m is obtained using the approach in [44] (see also [45]), giving

$$\mathscr{Z}(m) \simeq C\Lambda_{\max}^{m}, \tag{39}$$

where C is a constant and (assuming no cooperativity effects [44, 21]) $\Lambda_{\max}$ is the largest root Λ to the algebraic equation

$$\Lambda^{\lambda} - \Lambda^{\lambda-1} - \kappa = 0. \tag{40}$$

The equation above is of order λ, i.e., the order is determined by the size of the chaperones. Introducing equation (39) in equation (38) we find that the mean first passage time for very large M approaches

$$\tau\,|_{M\gg 1} \to \tau_{\mathrm{ad}} = k^{-1}\frac{\Lambda_{\max}}{\Lambda_{\max}-1}(M+1), \tag{41}$$

which proves that for large chain lengths the adiabatic result for τ scales as M, just as for ratchet dynamics, but in general with a smaller prefactor than for ratchet motion. For the case of weak binding, κ small, so that $\ln\Lambda_{\max} \ll 1$ we can write equation (41) according to $\tau \approx k^{-1}\ln\Lambda_{\max}^{-1}(M+1)$, so that $\tau \propto \ln\Lambda_{\max}^{-1}$ in agreement with the results in [21].

For univalent binding ($\lambda = 1$) we solve equation (40) and find the explicit result $\Lambda_{\max} = (1+\kappa)$. Interestingly, the mean translocation time is then inversely proportional, $\tau \propto 1/f$, to the filling fraction, $f = \kappa/(1+\kappa)$, of the chain, see appendix C in [21]; since $0 \leqslant f \leqslant 1$ the translocation process is slower than for ratchet motion as it should be, compare equation (35). We note that $\tau_{\mathrm{ad}}/\tau_{\mathrm{diff}} = 2(1+\kappa^{-1})/M$; see equations (33) and (41)[5]. For divalent binding ($\lambda = 2$) equation (40) becomes a second order algebraic equation, which can straightforwardly be solved, yielding $\Lambda_{\max} = [1+(1+4\kappa)^{1/2}]/2$. In figure 5 the result as contained in (41) is shown for the cases $\lambda = 1$ and 5; for the case $\lambda = 5$ the algebraic equation (40) is solved numerically.

We point out that, in contrast to the cases of slow binding and ratchet motion discussed in the previous subsections, for the fast binding and unbinding case (reversible binding [21]) considered here typically the larger part of the phase space is explored (see figure 3 (top)) before absorption. For fast (un)binding we define the effective force $F(m) = 2F_0(\tilde{t}^+(m) - \tilde{t}^-(m))/(\tilde{t}^+(m) + \tilde{t}^-(m))$, with $F_0 = k_{\mathrm{B}}T/\sigma$ as before. The force is illustrated in figure 3 (bottom), showing a constant value for large m; this asymptotic value is smaller than that for ratchet motion. Also, notice that for $\lambda = 5$ the force oscillates with a period $\approx \lambda$ for smaller m in agreement with [21].

[5] The corresponding result for a Brownian ratchet is $\tau_{\mathrm{ad}}/\tau_{\mathrm{diff}} = (1+2\kappa^{-1})/M$. The difference has the same origin as discussed in section 5.2.

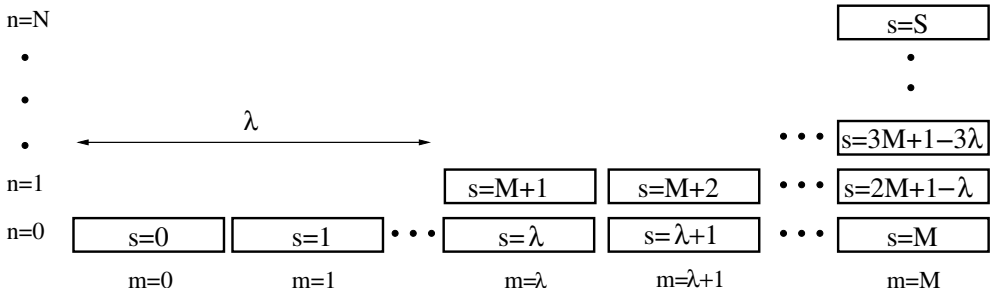

Figure 4. Enumeration scheme for the numerical analysis: the two-dimensional grid points (m, n) are replaced by a one-dimensional running variable s. See the text for details.

5.4. General case, numerical analysis

To solve the eigenvalue equation (13) by a numerical scheme, it is convenient to replace the two-dimensional grid points (m, n) by a one-dimensional coordinate s counting all lattice points; compare [28] and [40]. We choose the enumeration illustrated in figure 4. From this figure we notice that $n \in [0, N]$ (where $N = [M/\lambda]$) and that $m \in [n\lambda, M]$. An arbitrary s-point can be obtained from a specific (m, n) according to

$$s = n(M+1) - \sum_{n'=1}^{n} n'\lambda + m = n(M+1) - \frac{n(n+1)}{2}\lambda + m. \tag{42}$$

From this relation we notice that the maximum s value is

$$S = \max\{s\} = (N+1)\left(M + 1 - \frac{N\lambda}{2}\right) - 1. \tag{43}$$

Expression (42) allows us to change the transfer coefficients to the s-variable, $\mathsf{t}^{\pm}(m, n) \to \mathsf{t}^{\pm}(s)$ and $\mathsf{r}^{\pm}(m, n) \to \mathsf{r}^{\pm}(s)$, using the explicit expressions (25)–(28) for the transfer coefficients, together with the boundary conditions in equations (4), (5), (7) and (8). From equation (42) and figure 4 we notice that a local jump in the m-direction also corresponds to a local jump in s-space, i.e., that

$$\begin{aligned} &m \to m-1 \Longleftrightarrow s \to s-1|_{1\leqslant m\leqslant M}, \\ &m \to m+1 \Longleftrightarrow s \to s+1|_{0\leqslant m\leqslant M-1}. \end{aligned} \tag{44}$$

However, a jump in the n-direction is equal to a non-local jump in s-space:

$$\begin{aligned} &n \to n-1 \Longleftrightarrow s \to s-\Delta s^{-}|_{1\leqslant n\leqslant n^{\max}(m)}, \\ &n \to n+1 \Longleftrightarrow s \to s+\Delta s^{+}|_{0\leqslant n\leqslant n^{\max}(m)-1}, \end{aligned} \tag{45}$$

with $\Delta s^{-} = M + 1 - n\lambda$ and $\Delta s^{+} = M + 1 - (n+1)\lambda$. Using the results above, we find that the eigenvalue problem (13) can be written in matrix form as

$$\sum_{s'} W(s, s')\, Q_p(s') = -\eta_p\, Q_p(s) \tag{46}$$

where explicitly the matrix elements are

$$\begin{aligned} W(s, s-1) &= \mathsf{t}^{+}(s-1), && \text{for } s \pitchfork 1 \leqslant m \leqslant M, \\ &= 0, && \text{for } s \pitchfork m = n\lambda \wedge n = n^{\max}(m) \\ W(s, s+1) &= \mathsf{t}^{-}(s+1), && \text{for } s \pitchfork 0 \leqslant m \leqslant M-1 \\ W(s, s-\Delta s^{-}) &= \mathsf{r}^{+}(s-\Delta s^{-}), && \text{for } s \pitchfork 1 \leqslant n \leqslant n^{\max}(m), \\ W(s, s+\Delta s^{+}) &= \mathsf{r}^{+}(s+\Delta s^{+}), && \text{for } s \pitchfork 0 \leqslant n \leqslant n^{\max}(m)-1, \\ W(s, s) &= -(\mathsf{t}^{+}(s) + \mathsf{t}^{-}(s) + \mathsf{r}^{+}(s) + \mathsf{r}^{-}(s)), \end{aligned} \tag{47}$$

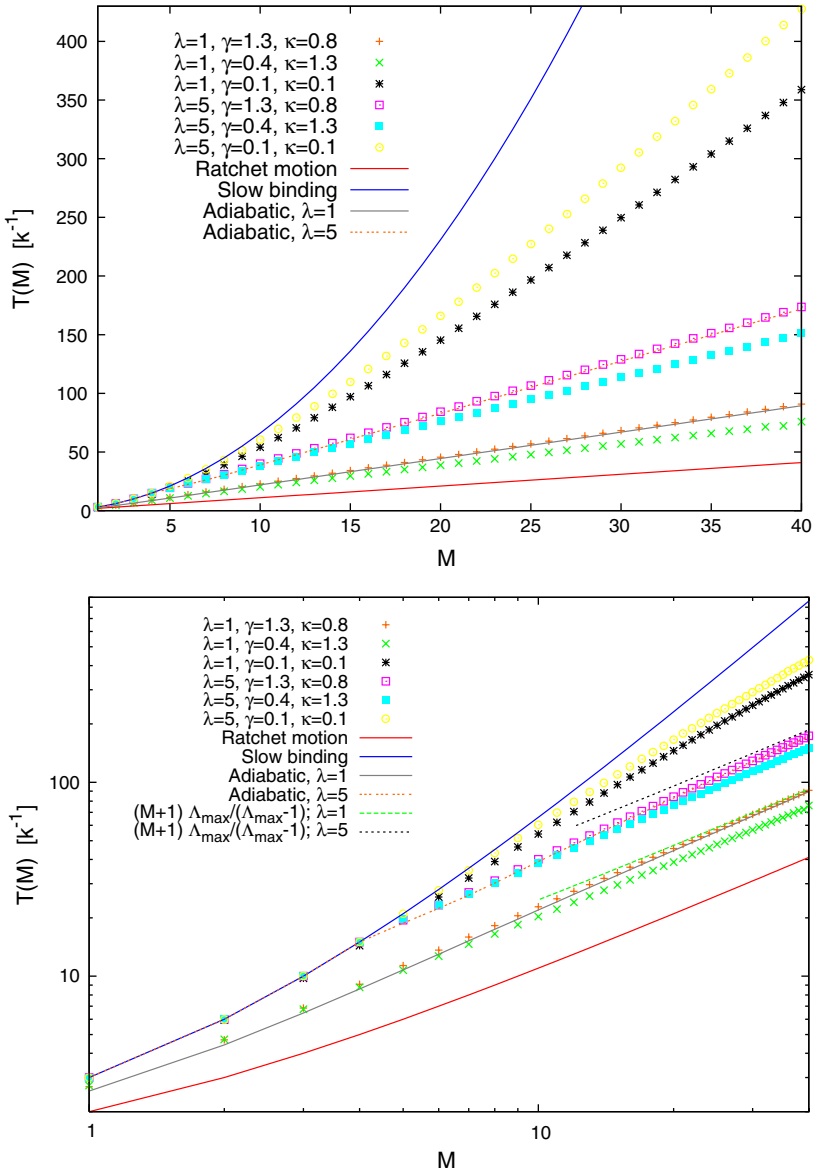

Figure 5. Mean translocation time τ as a function of M, using (top) linear axes; (bottom) logarithmic axes. Results are shown for (i) slow binding, equation (33); (ii) the ratchet result, equation (35); (iii) fast (un)binding, equation (38) for different sizes of the chaperones (here $\lambda = 1$ and 5 respectively) with binding strength $\kappa = 0.8$. Also, results are shown for (iv) the general dynamics, as obtained by numerically inverting the transfer matrix (47) and using the mean first passage time expression (19). In addition, in the bottom graph the large M result (41) is shown.

and the remaining matrix elements are equal to zero. We have introduced the notation $s \pitchfork$ with the meaning 's is to be taken for'. Notice that (with the present enumeration scheme) the tridiagonal part of the W-matrix is determined by jumps in the m-direction, i.e., by t^+ and t^-, whereas elements outside of the tridiagonal part are determined by r^+ and r^-. The problem

at hand is that of determining the eigenvalues and eigenvectors of the $(S+1)\times(S+1)$-matrix W above. Convenient checks of the numerical results include the following: (i) the eigenvalues should be real and negative (so that $\eta_p > 0$); (ii) the eigenvectors should satisfy the orthonormality relation, equation (A.3).

In figure 5 we show results for the mean translocation time. From the results of the previous section we see that for ratchet motion (section 5.2) as well as for fast binding and unbinding dynamics (section 5.3) the mean translocation time scales as $\simeq M$. For slow binding as discussed in section 5.1 we have that τ scales as $\simeq M^2$ for large M. The general results shown in figure 5 are obtained by numerically solving the eigenvalue equation (46), and using the mean first passage time expression (19). All results are shown for the case of small chaperones, $\lambda = 1$, and for larger chaperones, $\lambda = 5$. We notice the slow binding result (33) and the ratchet results (35) constitute upper and lower limits to the general mean translocation time τ. Also, the approach to the very large M result (41) is rather slow, due to finite size effects.

We point out that even though our main focus here has been to calculate the mean first passage time τ, any quantity of interest (such as, for instance, the mean first passage time density $f(t)$, see section 3), can be obtained from the solution of the eigenvalue problem presented in this section.

6. Conclusions and discussion

In this study the translocation of a stiff polymer consisting of M monomers through a nanopore in a membrane was investigated in the presence of binding particles (chaperones) that bind onto the polymer. Our $(2+1)$-variable master equation governing the coupling of the random biopolymer passage and the random chaperone (un)binding is an extension of a previous continuum Fokker–Planck approach [11]. From our approach three limiting regimes emerge:

(i) for the case of slow binding the motion is purely diffusive, and the mean translocation time τ scales as $\tau \simeq M^2$ for large M;
(ii) for fast binding but slow unbinding the motion is ratchet-like, for small chaperones $\lambda = 1$, and $\tau \simeq M$;
(iii) for the case of fast binding and unbinding dynamics, we performed the adiabatic elimination of the fast variable n, and find that for a very long polymer $\tau \simeq M$, but with a smaller prefactor than for ratchet-like dynamics.

We point out that our approach is the first, to our knowledge, that is able to account for (the approach towards) these three limiting regimes within a single framework. For the intermediate cases our scheme is solved numerically, which requires numerically inverting the transfer matrix W (of approximate size $M^2 \times M^2$), for which an explicit expression is given.

Let us summarize the essential differences between our approach compared to the original Brownian ratchet ideas in [14, 15].

(1) In this reference the polymer motion through the pore was characterized by continuous diffusion. In contrast, we assume that the motion proceeds through random jumps of finite step length, as appropriate, for instance, for a polymer moving through a saw-tooth-like pore potential, as suggested in [23] for explaining the surprisingly large translocation times for DNA translocation.
(2) In [14, 15] the chaperones bind independently along the polymer. Here, we include the fact that typically chaperones are larger than the size of a monomer, giving rise to a 'car parking effect'.

(3) We here consider arbitrary ratios of the relevant (un)binding rate and the diffusive rate—this is in contrast to the results in [14, 15] where only the cases of Brownian ratchet motion and fast (un)binding dynamics were considered.

An implicit assumption in our study is that the number of binding proteins in the bath surrounding the translocating chain is large (but of finite concentration); see [21], appendix B. In other words, we assume that the diffusion of the chaperones in volume is fast in comparison to the timescales of translocation and chaperone (un)binding dynamics (well mixing condition). Thus, chaperone bath depletion effects, that may occur for a finite number of chaperones [11], are not present in this study. We note that we have not explicitly included chain flexibility into the present scheme. We have also assumed that the binding energy is the same along the polymer, and that the major friction for the polymer originates from interactions in the pore (we hence neglected hydrodynamic friction from the polymer part sticking out of the pore). Although each of these effects may be relevant to experimental situations of chaperone-driven translocation, here we focused on the pure chaperone effect. Note that one efficient way to include additional details in the translocation scenario is the stochastic simulation technique based on the Gillespie algorithm [46, 47]. It would also be interesting to compare the results from this study with Brownian dynamics simulations along similar lines as in [11], but with the (realistically) large chaperones considered here.

We finally point out that the coupled dynamics studied here is a generic example of how a stochastic process can rectify another one. Our (2 + 1)-variable master equation formalism provides a general framework for treating such rectification processes, that may also be useful in other fields.

Appendix A. Proof of the orthogonality and the negativity of eigenvalues

In this appendix we prove an orthonormality relation for the eigenvectors $Q_p(s)$ and that the corresponding eigenvalues $-\eta_p$ are negative; see equation (46).

In terms of the running variable s, see equation (42), and the W-matrix defined in equation (47) the detailed balance conditions (9) and (10) can be written as

$$W(s,s')P^{\rm st}(s') = W(s',s)P^{\rm st}(s), \tag{A.1}$$

for $s \neq s'$; we note that the equation above holds trivially also for $s = s'$. Here, $P^{\rm st}(s) = \mathscr{Z}(s)/\mathscr{Z}$ with $\mathscr{Z}(s)$ being the partition coefficient and $\mathscr{Z} = \sum_s \mathscr{Z}(s)$.

To derive the orthogonality relation from the detailed balance condition (A.1), consider the expression

$$\begin{aligned}
-(\eta_p - \eta_{p'}) \sum_s \frac{Q_p(s)Q_{p'}(s)}{P^{\rm st}(s)} &= \sum_{s,s'} \frac{W(s,s')Q_p(s')Q_{p'}(s)}{P^{\rm st}(s)} - \sum_{s,s'} \frac{Q_p(s)W(s,s')Q_{p'}(s')}{P^{\rm st}(s)} \\
&= \sum_{s,s'} \frac{W(s,s')Q_p(s')Q_{p'}(s)}{P^{\rm st}(s)} - \sum_{s,s'} \frac{W(s',s)Q_p(s)Q_{p'}(s')}{P^{\rm st}(s')} = 0
\end{aligned} \tag{A.2}$$

where we used equation (46), and the detailed balance condition (A.1). Therefore, the orthogonality relation

$$\sum_s \frac{Q_p(s)Q_{p'}(s)}{P^{\rm st}(s)} = \delta_{p,p'}, \tag{A.3}$$

follows. Returning to the double index (m, n), this is equivalent to the statement

$$\sum_{m,n} \frac{Q_p(m,n)Q_{p'}(m,n)}{P^{\mathrm{st}}(m,n)} = \delta_{p,p'} \tag{A.4}$$

for the eigenfunctions $Q_p(m, n)$.

To prove that all the eigenvalues are negative it is convenient to separate the W-matrix into the corresponding reflective matrix $W_{\mathrm{r}}(s, s')$ and the additional absorbing terms

$$W(s, s') = W_{\mathrm{r}}(s, s') - w_{\mathrm{a}}(s)\delta_{s,s'}, \tag{A.5}$$

where the absorbing part is

$$w_{\mathrm{a}}(s) = -\sum_{s'} W(s', s). \tag{A.6}$$

It follows from equation (47) that

$$w_{\mathrm{a}}(s) \geqslant 0, \tag{A.7}$$

with at least one of the $w_{\mathrm{a}}(s)$ strictly greater than zero, and

$$\sum_{s} W_{\mathrm{r}}(s, s') = 0, \tag{A.8}$$

which is the condition that probability is conserved when there are no absorbing terms. Note that it does not matter for the detailed balance conditions, equation (A.1), that the diagonal of the W-matrix is modified. Therefore detailed balance is also satisfied for the reflective matrix: $W_{\mathrm{r}}(s, s')P^{\mathrm{st}}(s') = W_{\mathrm{r}}(s', s)P^{\mathrm{st}}(s)$. This detailed balance condition together with equation (A.8) guarantees that $P^{\mathrm{st}}(s)$ is an eigenvector of the W_{r}-matrix with zero eigenvalue [37]. Furthermore, since the system is ergodic, i.e. it is possible for the system to reach any state from any other state, any eigenvector of W_{r} with zero eigenvalue will be proportional to $P^{\mathrm{st}}(s)$ [37]. The negativity of the eigenvalues $-\eta_p$ then follows because

$$\begin{aligned} -\eta_p &= \sum_{s,s'} \frac{W(s, s')Q_p(s')Q_p(s)}{P^{\mathrm{st}}(s)} \\ &= \sum_{s,s'} \frac{W_{\mathrm{r}}(s, s')Q_p(s')Q_p(s)}{P^{\mathrm{st}}(s)} - \sum_{s} \frac{Q_p(s)^2}{P^{\mathrm{st}}(s)} w_{\mathrm{a}}(s) < 0. \end{aligned} \tag{A.9}$$

The first term after the last equality sign is non-positive since the W_{r}-matrix is negative semi-definite [37]. The only possibility for this term to be zero is that $Q_p(s)$ is proportional to $P^{\mathrm{st}}(s)$. In this case, however, the last term will be strictly negative because at least one of the $w_{\mathrm{a}}(s)$ is non-zero.

Appendix B. Mean first passage time

For a one-variable master equation with reflecting boundary condition at $m = 0$ and absorbing boundary condition at $m = M + 1$, and with transfer coefficient $t^+(m)$ ($t^-(m)$) in the forward (backward) direction, the mean first passage time is given by the explicit expression (see [38], chapter 7.4)

$$\mathsf{T} = \sum_{m=0}^{M} \Phi(m) \sum_{m'=0}^{m} \frac{1}{\mathsf{t}^+(m')\Phi(m')}, \tag{B.1}$$

where

$$\Phi(m) = \prod_{j=1}^{m} \frac{\mathsf{t}^-(j)}{\mathsf{t}^+(j)} \tag{B.2}$$

and we have assumed that initially $m = 0$. If we invoke the detailed balance condition $\mathsf{t}^+(m-1)\mathscr{Z}(m-1) = \mathsf{t}^-(m)\mathscr{Z}(m)$, for $m = 1, \ldots M$, where $\mathscr{Z}(m)$ is the partition coefficient, equation (B.1) reduces to

$$\mathsf{T} = \sum_{m=0}^{M} \frac{1}{\mathsf{t}^+(m)\mathscr{Z}(m)} \sum_{m'=0}^{m} \mathscr{Z}(m'). \tag{B.3}$$

The expressions above are used in section 5.

References

[1] Alberts B, Roberts K, Bray D, Lewis J, Raff M and Watson J D 1994 *The Molecular Biology of the Cell* (New York: Garland)
[2] Henrikson S E, Misakian M, Robertson B and Kasianowicz J J 2000 *Phys. Rev. Lett.* **85** 3057
[3] Meller A, Nivon L and Branton D 2001 *Phys. Rev. Lett.* **86** 3435
[4] Gerland U, Bundschu R and Hwa T 2004 *Phys. Biol.* **1** 19
[5] Kasianowicz J J, Henrickson S E, Weetall H H and Robertson B 2001 *Anal. Chem.* **73** 2268
[6] Ambjörnsson T and Metzler R 2005 *J. Comput. Theor. Nanosci.* **2** 389
[7] Di Marzio E and Kasianowicz J J 2003 *J. Chem. Phys.* **119** 6378
[8] Storm A J, Chen J H, Ling X S, Zandbergen H W and Dekker A 2005 *Nat. Mater.* **2** 537
[9] Meller A 2003 *J. Phys.: Condens. Matter* **15** R581
[10] Bates M, Burns M and Meller A 2003 *Biophys. J.* **84** 2366
[11] Zandi R, Reguera D, Rudnick J and Gelbart W M 2003 *Proc. Natl Acad. Sci. USA* **100** 8649
[12] Liebermeister W, Rapoport T A and Heinrich R 2001 *J. Mol. Biol.* **305** 643
[13] Elston T C 2000 *Biophys. J.* **79** 2235
Elston T C 2002 *Biophys. J.* **82** 1239
[14] Simon S F, Peskin C S and Oster G F 1992 *Proc. Natl Acad. Sci. USA* **89** 3770
[15] Peskin C S, Odell G M and Oster G F 1993 *Biophys. J.* **65** 316
[16] Chauwin J-F, Oster G and Glick B S 1998 *Biophys. J.* **74** 1732
[17] Matlack K E S, Mothes W and Rapoport T A 1998 *Cell* **92** 381
Matlack K E S, Misselwitz B, Plath K and Rapoport T A 1999 *Cell* **97** 553
[18] Neupert W and Brunner M 2002 *Nat. Rev. Mol. Cell Biol.* **3** 555
[19] Salman H, Zbaida D, Rabin Y, Chatenay D and Elbaum M 2001 *Proc. Natl Acad. Sci. USA* **98** 7247
[20] Farkas Z, Derényi I and Vicsek T 2003 *J. Phys.: Condens. Matter* **15** 1767
[21] Ambjörnsson T and Metzler R 2004 *Phys. Biol.* **1** 77
[22] Sung W and Park P J 1996 *Phys. Rev. Lett.* **77** 783
[23] Lubensky D K and Nelson D R 1999 *Biophys. J.* **77** 1824
[24] Muthukumar M 1999 *J. Chem. Phys.* **111** 10371
[25] Muthukumar M 2001 *Phys. Rev. Lett.* **86** 3188
[26] Kafri Y, Lubensky D K and Nelson D R 2004 *Biophys. J.* **86** 3373
[27] Ambjörnsson T and Metzler R 2005 *Phys. Rev.* E **72** 030901(R)
[28] Ambjörnsson T and Metzler R 2005 *J. Phys.: Condens. Matter* **17** S1841
[29] Chuang J, Kantor Y and Kardar M 2001 *Phys. Rev.* E **65** 011802
[30] Kantor Y and Kardar M 2004 *Phys. Rev.* E **69** 021806
[31] Metzler R and Klafter J 2003 *Biophys. J.* **85** 2776
[32] Metzler R and Klafter J 2004 *J. Phys. A: Math. Gen.* **37** R161
[33] Flomenbom O and Klafter J 2003 *Phys. Rev.* E **68** 041910
[34] Flomenbom O and Klafter J 2004 *Biophys. J.* **86** 3576
[35] Ambjörnsson A, Apell S P, Konkoli Z, Di Marzio E and Kasianowicz J J 2002 *J. Chem. Phys.* **117** 4063
[36] Kolomeisky A and Slonkina E 2003 *J. Chem. Phys.* **118** 7112
[37] van Kampen N G 1992 *Stochastic Processes in Physics and Chemistry* (Amsterdam: North-Holland)
[38] Gardiner C W 1996 *Handbook of Stochastic Methods for Physics, Chemistry and the Natural Sciences* (Berlin: Springer)
[39] Risken H 1989 *The Fokker–Planck Equation* (Berlin: Springer)
[40] Press W H, Teukolsky S A, Vetterling W T and Flannery B P 1992 *Numerical Recipes in C* 2nd edn (Cambridge: University Press)
[41] McQuistan R B 1968 *Nuovo Cimento* **LVIII** 86

[42] Epstein I R 1978 *Biophys. Chem.* **8** 327
[43] Harada Y, Funatsu T, Murakami K, Nonoyama Y, Ishihama A and Yanagida T 1999 *Biophys. J.* **76** 709
[44] Di Cera E and Kong Y 1996 *Biophys. Chem.* **61** 107
[45] Kong Y 2001 *J. Phys. Chem.* B **105** 10111
[46] Gillespie D T 1976 *J. Comput. Phys.* **22** 403
Gillespie D T 1977 *J. Phys. Chem.* **81** 2340
[47] Banik S K, Ambjörnsson T and Metzler R 2005 *Europhys. Lett.* **71** 852